

# Relativistic electron scattering by electromagnetic ion cyclotron fluctuations: test particle simulations

K. Liu,<sup>1</sup>D. S. Lemons,<sup>2</sup> D. Winske,<sup>1</sup> and S. P. Gary<sup>1</sup>

---

K. Liu, Los Alamos National Laboratory, Los Alamos, NM 87545, USA.(kaijun@lanl.gov)

D. S. Lemons, Department of Physics, Bethel College, North Newton, Kansas, 67117, USA.(dlemons@bethelks.edu)

D. Winske, Los Alamos National Laboratory, Los Alamos, NM 87545, USA.(winske@lanl.gov)

S. P. Gary, Los Alamos National Laboratory, Los Alamos, NM 87545, USA.(pgary@lanl.gov)

<sup>1</sup>Los Alamos National Laboratory, Los Alamos, NM 87545, USA.

<sup>2</sup>Department of Physics, Bethel College, North Newton, Kansas, 67117, USA.

**Abstract.** Relativistic electron scattering by electromagnetic ion cyclotron (EMIC) fluctuations is studied using test particle computations coupled to a hybrid simulation code. The enhanced EMIC fluctuations are derived from a one-dimensional, self-consistent hybrid simulation model and is due to the growth of the ion cyclotron instability driven by the ion temperature anisotropy,  $T_{i\perp} > T_{i\parallel}$ , in a magnetized, homogeneous, collisionless plasma with a single ion species. The test particle computations follow the motion of relativistic test electron particles in the input EMIC fluctuations. The time evolution of the mean-square pitch-angle change is calculated and used to estimate the pitch-angle diffusion coefficient. Finally the results are compared with quasi-linear diffusion theory. The present study has applications to relativistic electron dynamics in the terrestrial magnetosphere.

## 1. Introduction

Relativistic electrons, namely those with energies above 1 MeV, trapped in the Van Allen radiation belts are a serious threat to the operation of spacecraft in the terrestrial magnetosphere and have drawn increasing attention over the past decade [*Baker, 2002*]. The fluxes of such electrons are highly variable, especially during geomagnetic storms [*Friedel et al., 2002*]. The variability of the relativistic electrons is due to a competition between various loss and source processes [*Reeves et al., 2003*]. Understanding these processes is essential to the study of the radiation belts.

Electrons in the radiation belts undergo three types of periodic motion (gyration, bounce, and drift). Each of them corresponds to an adiabatic invariant, usually referred to as the 1st, 2nd, and 3rd invariants, respectively [*Schulz and Lanzerotti, 1974*]. Wave-particle interactions, in particular electron gyroresonance with ELF, VLF, and electromagnetic ion cyclotron (EMIC) waves, can violate the 1st and 2nd adiabatic invariants and produce local acceleration and pitch-angle scattering of charged particles [*Summers et al., 1998; Reeves et al., 2003; Meredith et al., 2004; Shprits, 2009*]. The pitch-angle scattering may transport charged particles into the loss cone where they are removed by collisions with atmospheric particles [*Imhof, 1968; Selesnick et al., 2003*].

Gyroresonant wave-particle interactions in the radiation belts have been usually studied in terms of quasi-linear theory [*Kennel and Engelmann, 1966; Lerche, 1968*]. According to this theory, the dynamics of radiation-belt particles is described by a Fokker-Planck-type diffusion equation [*Summers, 2005*]. The diffusion coefficients in the diffusion equation depend on the wave spectra and plasma properties. The evaluation of the diffusion co-

efficients has been the focus of numerous studies [*Lyons et al.*, 1971; *Albert*, 2003, 2005; *Glauert and Horne*, 2005; *Summers and Thorne*, 2003; *Summers*, 2005]. It has been found that gyroresonant interactions with waves at frequencies well below the resonant particles' gyrofrequency result in diffusion primarily in pitch angle, while interactions with waves at frequencies comparable with, or greater than, the resonant particle's gyrofrequency can cause diffusion in energy at rates comparable with or greater than pitch-angle diffusion rates [*Kennel and Engelmann*, 1966; *Lyons*, 1974]. The present study concentrates on the gyroresonant interactions of relativistic electrons with EMIC waves at propagation parallel to the background magnetic field, for which pitch-angle scattering dominates.

EMIC waves with typical amplitudes of 1 to 10 nT are commonly present in the outer radiation belts [*Meredith and Anderson*, 2003; *Fraser and Nguyen*, 2001]. They are excited by the anisotropic ( $T_{i\perp} > T_{i\parallel}$ , where the subscripts denote directions relative to the background geomagnetic field) distribution of ring current ions [*Cornwall*, 1965; *Mauk and McPherron*, 1980; *Anderson et al.*, 1996]. The equatorial region along the high-density duskside plasmopause is a preferred region for EMIC wave excitation [*Horne and Thorne*, 1993; *Fraser and Nguyen*, 2001]. EMIC waves propagate at frequencies below the proton gyrofrequency and can resonate with relativistic electrons to cause pitch-angle scattering and, consequently, precipitation loss to the atmosphere. Observations show direct evidence of the link between relativistic electron losses and EMIC waves [*Millan and Thorne*, 2006].

Quasi-linear theory has been very successful in the study of radiation-belt particle dynamics [*Kennel and Petschek*, 1966; *Lyons et al.*, 1972; *Thorne et al.*, 2005]. However, quasi-linear theory has its natural limits owing to the weak turbulence approximation and

the assumption of a uniformly-magnetized, homogeneous, collisionless background plasma involved in its derivation [Kennel and Engelmann, 1966]. Using a test particle code, the present study aims to understand the scattering processes at a more fundamental level. The test particle code follows the motion of relativistic test electron particles under any arbitrary input EMIC fluctuations. The time evolution of the mean-square pitch-angle change of the electrons is then calculated and used to estimate the pitch-angle diffusion coefficient. Finally the results are compared with quasi-linear diffusion theory. The present simulations are carried out in 1D (one spatial dimension, but all three velocity components retained), i.e., only field-aligned EMIC waves are involved.

This paper is organized as follows: section 2 introduces the results of quasi-linear diffusion theory on relativistic electron scattering by field-aligned EMIC waves and proposes a method to calculate the the pitch-angle diffusion coefficient directly from the test particle simulations; section 3 briefly describes the simulation model and presents the simulation results; we discuss the results in section 4; and the conclusions are summarized in section 5.

## 2. Quasi-linear Diffusion Theory

For field-aligned EMIC waves, the electron diffusion is essentially in pitch angle only and can be described by a pure pitch-angle diffusion equation,

$$\frac{\partial f(\alpha, t)}{\partial t} = \frac{1}{\sin \alpha} \frac{\partial}{\partial \alpha} \left( D_{\alpha\alpha} \sin \alpha \frac{\partial f(\alpha, t)}{\partial \alpha} \right), \quad (1)$$

where,  $\alpha$  is pitch angle,  $t$  is time,  $f(\alpha, t)$  is the spatially uniform, zeroth-order, gyrophase-averaged electron distribution function and  $\int_0^\pi f(\alpha, t) \sin \alpha d\alpha = 1$ , and  $D_{\alpha\alpha}$  is the pitch-angle diffusion coefficient, which is in general a function of  $\alpha$ .

The rigorously exact diffusion coefficients, within the limits of quasi-linear theory, for parallel-propagating electromagnetic waves of general spectral density  $W(k)$  have been given by *Summers* [2005] (equations (17)-(19) and (27)-(28)). The evaluation of these expressions requires the dispersion relation for field-aligned (L-mode) EMIC waves and the resonance condition. The resonance condition for relativistic electrons with parallel-propagating L-mode EMIC waves of frequency  $\omega$  and wave number  $k$  is,

$$\omega - kv_{\parallel} = -\Omega_e/\gamma, \quad (2)$$

where  $\gamma = 1/\sqrt{1 - v^2/c^2}$  is the Lorentz factor,  $c$  is the light speed,  $v = \sqrt{v_{\parallel}^2 + v_{\perp}^2}$  is the electron speed,  $\Omega_e = eB_0/m_e$  ( $e$  is the electron charge in absolute value,  $B_0$  is the background magnetic field) is the electron gyrofrequency. The first term  $\omega$  on the left-hand side can be safely neglected in equation (2) for relativistic electron resonant interactions with field-aligned EMIC waves, so

$$kv_{\parallel} = \Omega_e/\gamma. \quad (3)$$

Equation (3) requires electrons to be “co-streaming” with EMIC waves in order to have resonance, which is opposite to the usual requirement for resonance with field-aligned whistler waves, as noticed by *Albert and Bortnik* [2009]. Furthermore, equation (3) defines a minimum wavenumber  $k_{min} = \Omega_e/\gamma v$  that only wave modes with  $k > k_{min}$  can resonate with electrons of given energy.

The neglecting of  $\omega$  in equation (3) makes the dispersion relation for field-aligned EMIC waves not needed in evaluating the pitch-angle diffusion coefficient given by *Summers* [2005] for relativistic electron scattering by parallel-propagating EMIC fluctuations. The

pitch-angle diffusion coefficient simplifies to,

$$D_{\alpha\alpha}(\alpha) = \frac{\pi}{2} \frac{\Omega_e}{\gamma} \frac{kW(k)}{W_0}, \quad (4)$$

where  $k$  is the resonant wavenumber given by equation (3),  $W(k)$  is the wave magnetic field spectral density defined by,

$$W_{tot} = \int_{k_1}^{k_2} W(k) dk, \quad (5)$$

$W_{tot}$  is the total wave magnetic energy density, and  $W_0$  is the background magnetic field energy density. Equation (4) is the same as the approximate expression in the work of *Summers and Thorne* [2003] (equation (8)) except for the extra factor  $\pi/2$ , which has also been noticed by *Summers* [2005].

In the following part, we derive an expression which enables us to determine  $D_{\alpha\alpha}$  from the results of our test-particle computations. If  $f(\alpha, t = 0) = \delta(\alpha - \alpha_0)/\sin \alpha_0$  is assumed ( $1/\sin \alpha_0$  is a normalization factor), then from equation (1), the time derivative of the mean-square pitch-angle change is given by,

$$\begin{aligned} \frac{\partial \overline{\Delta\alpha^2}}{\partial t} &= \frac{\partial \int_0^\pi (\alpha - \alpha_0)^2 f(\alpha, t) \sin \alpha d\alpha}{\partial t} \\ &= \int_0^\pi (\alpha - \alpha_0)^2 \sin \alpha \frac{\partial f(\alpha, t)}{\partial t} d\alpha \\ &= \int_0^\pi (\alpha - \alpha_0)^2 \frac{\partial}{\partial \alpha} \left( D_{\alpha\alpha} \sin \alpha \frac{\partial f(\alpha, t)}{\partial \alpha} \right) d\alpha \\ &= (\alpha - \alpha_0)^2 D_{\alpha\alpha} \sin \alpha \frac{\partial f(\alpha, t)}{\partial \alpha} \Big|_0^\pi \\ &\quad - 2(\alpha - \alpha_0) D_{\alpha\alpha} \sin \alpha f(\alpha, t) \Big|_0^\pi \\ &\quad + 2 \int_0^\pi D_{\alpha\alpha} f(\alpha, t) \sin \alpha d\alpha \\ &\quad + 2 \int_0^\pi (\alpha - \alpha_0) D_{\alpha\alpha} f(\alpha, t) \cos \alpha d\alpha \\ &\quad + 2 \int_0^\pi (\alpha - \alpha_0) f(\alpha, t) \frac{\partial D_{\alpha\alpha}}{\partial \alpha} \sin \alpha d\alpha \end{aligned} \quad (6)$$

If  $f(\alpha, t)$  and  $\frac{\partial f(\alpha, t)}{\partial \alpha}$  are finite at  $\alpha = 0, \pi$ , which generally is true, the first two terms are 0. The last term appears if the diffusion coefficient has dependence on  $\alpha$ . If  $D_{\alpha\alpha}$  is a constant for simplicity, Equation (6) becomes,

$$\frac{\partial \overline{\Delta\alpha^2}}{\partial t} = 2D_{\alpha\alpha} + 2D_{\alpha\alpha} \int_0^\pi (\alpha - \alpha_0) f(\alpha, t) \cos \alpha d\alpha. \quad (7)$$

Interestingly, besides the expected first term similar to the Einstein relation for Brownian motion [Ivanov, 1965; Lemons, 2002], equation (7) has an extra term on the right-hand side. The extra term causes the time evolution of the mean-square pitch-angle change to depart from a linear growth with time. This departure can be easily verified by solving the pitch-angle diffusion equation numerically (not shown).

The last two terms in equation (6) both have a factor of  $(\alpha - \alpha_0)f(\alpha, t)$ . Their contribution is negligible in the early stage when  $f(\alpha, t)$  has not spread significantly from the initial  $f(\alpha, t = 0) = \delta(\alpha - \alpha_0)/\sin \alpha_0$ . Therefore, equation (6) simplifies to,

$$\frac{\partial \overline{\Delta\alpha^2}}{\partial t} = 2 \int_0^\pi D_{\alpha\alpha} f(\alpha, t) \sin \alpha d\alpha \approx 2D_{\alpha\alpha}(\alpha_0). \quad (8)$$

Equation (8) suggests that, in the early stage, the mean-square pitch-angle change grows approximately linearly with time and the pitch-angle diffusion coefficient can be estimated from the growth rate,

$$D_{\alpha\alpha}(\alpha_0) = \frac{\overline{\Delta\alpha^2}(t_2) - \overline{\Delta\alpha^2}(t_1)}{2\Delta t}, \quad (9)$$

where  $\Delta t = t_2 - t_1$ .

After the early stage,  $f(\alpha, t)$  spreads from the initial  $f(\alpha, 0) = \delta(\alpha - \alpha_0)/\sin \alpha_0$ . The contribution of the last two terms in equation (6) increases. The time evolution of the mean-square pitch-angle change begins to depart from a linear growth significantly. Technically, the time this significant departure happens, referred to as the departure time,  $\tau_d$ ,

gives the maximum of  $\Delta t$  to estimate the diffusion coefficient using equation (9). On the other hand, in analogy to the concept of the finite correlation time of particle velocity in Brownian motion [*Ivanov, 1965*], the pitch-angle change at every small time increment is random only when the time-increment length is above a finite correlation time,  $\tau_c$ .  $\tau_c$  gives the minimum time limit when a linear growth of the mean-square pitch-angle change can be expected. At  $t < \tau_c$ , the scattering process is not stochastic and cannot be described by a Fokker-Planck-type diffusion equation. Naturally,  $\tau_c \ll \tau_d$  is required for equation (1) to be applicable.  $\tau_c < t < \tau_d$  gives the time range during which the mean-square pitch-angle change grows linearly with time and equation (9) can be used to calculate the pitch-angle diffusion coefficient from the test particle simulations.

### 3. Test Particle Simulations

A test particle code has been developed to study pitch-angle diffusion by EMIC waves. The code allows arbitrary EMIC wave input and follows the motion of relativistic test electron particles using the particle-in-cell technique and the relativistic version of the Boris scheme [*Boris, 1970; Birdsall and Langdon, 1985*]. The time evolution of the mean-square pitch-angle change is then calculated and used to estimate the pitch-angle diffusion coefficient using equation (9).

In order to address the problem of relativistic electron scattering by EMIC waves in the radiation belts, the present study takes an EMIC wave input from a one-dimensional, self-consistent hybrid simulation model. The waves are generated from the ion cyclotron instability driven by the ion temperature anisotropy,  $T_{i\perp} > T_{i\parallel}$ , in a magnetized, homogeneous, collisionless, electron-proton plasma. A detailed description of the hybrid model was given by *Winske and Omidi* [1993]. The hybrid model has been successfully applied

to the study of the ion cyclotron instability [McKean *et al.*, 1992, 1994; Gary and Winske, 1996; Gary *et al.*, 1997].

The input EMIC waves for the present test particle simulation cases come from a one-dimensional hybrid simulation run. The simulation domain is in the direction of the background magnetic field  $B_0$ , that is, in the  $x$  direction. The system is periodic and its size is  $L_x = 2000\lambda_i$ , where  $\lambda_i = \sqrt{m_i/n_0\mu_0e^2}$  is the ion inertial length ( $n_0$  is the background plasma density). There are  $N_x = 2048$  grids and 100 ions in each grid.  $L_x = 2000\lambda_i$  and  $N_x = 2048$  are chosen so that there are enough wave modes to resonate with electrons in the test particle simulation. This is necessary because quasi-linear theory does not apply to a single wave mode [Kennel and Engelmann, 1966] and requires broad wave spectra. The other relevant input parameters are  $T_{i\perp}/T_{i\parallel} = 4.88$ ,  $\beta_{i\parallel} = 0.1$ , and  $c/V_A = 900$  where  $\beta_{i\parallel} = n_0T_{i\parallel}/(B_0^2/2\mu_0)$  and  $V_A = B_0/\sqrt{\mu_0n_0m_i}$  is the Alfvén velocity. In order to drive the ion cyclotron instability hard to get a good signal-to-noise ratio,  $T_{i\perp}/T_{i\parallel}$  is chosen to be large relative to its typical value ( $1.5 \sim 2$ ) in the ring current. One should also note that, in the hybrid simulation,  $T_{i\perp}/T_{i\parallel}$  drops to about 3 when the system reaches the quasi-steady state.

The waves generated by the above described hybrid simulation run are displayed in Figure 1. The top panel displays  $B_y/B_0$  versus  $x$  for  $0 \leq x \leq L_x/10 = 200\lambda_i$  at  $t = 75\Omega_i^{-1}$  ( $\Omega_i = eB_0/m_i$  is the proton gyrofrequency) when the system has reached a quasi-steady state. The bottom panel gives the spectral densities for  $B_y$ ,  $B_z$  components and the total EMIC waves (time averaged between  $t = 75\Omega_i^{-1}$  and  $t = 77\Omega_i^{-1}$ , during which the EMIC waves are taken as input for the test particle simulation cases displayed). As expected, the  $B_y$ ,  $B_z$  components have approximately the same spectral density. In addition, the

vertical dash line in the bottom panel marks the wavenumber  $k_{min} = \Omega_e/\gamma v = 0.42\lambda_i^{-1}$  above which the test electrons of 2MeV can resonate with the wave modes.  $k_{min}$  comes from the resonance condition equation (3), as discussed in section 2.

The test particle simulations use most of the simulation parameters from the above mentioned hybrid simulation which generates the input EMIC waves:  $L_x = 2000\lambda_i$ ,  $N_x = 2048$ ,  $c/V_A = 900$ . The test particle code also introduces a wave amplitude rescaling factor  $R$  so the EMIC wave amplitude can be freely adjusted to explore the effect of the wave amplitude on electron scattering. The effective wave spectral density in a test particle simulation is the input wave spectral density in Figure 1 multiplied by  $R^2$ . The system has 8000 test electrons, enough to make the present results statistically significant. The test electrons are initialized to have the same kinetic energy 2MeV, the same pitch angle  $\alpha_0$ , but random phase angle  $\theta$  and position  $x$ . The test particle code follows the motion of these electrons and gives the time evolution of the mean-square pitch-angle change. Figure 2 presents the time evolution of the mean-square pitch-angle change for electrons with different initial  $\alpha_0$  when the wave amplitude rescaling factor  $R = 0.05$ . During the time range shown in Figure 2, the time evolutions of the mean-square pitch-angle change for electrons with different initial  $\alpha_0$  are all close to a linear growth with time. Unlike the pitch angle but as expected from quasi-linear theory, the energy of each test electron does not change significantly [Kennel and Engelmann, 1966; Lyons, 1974].

Since the mean-square pitch-angle change for electrons with different initial  $\alpha_0$  in Figure 2 are all approximately linear in time, we take the mean-square pitch-angle changes at the beginning and the end of each run for simplicity (in these runs,  $\tau_c$  is negligible compared with  $\Delta t$ ), and estimate the pitch-angle diffusion coefficient using equation (9). The results

are shown in Figure 3 along with the diffusion coefficients given by quasi-linear theory equation (4) based on the total wave spectrum in Figure 1 with the wave amplitude rescaling factor  $R = 0.05$ . The diffusion coefficients given by the test particle simulation agree with the ones from quasi-linear theory very well. In addition, it is worth mentioning that the test electrons eventually reach a flat distribution ( $f(\alpha) = \text{constant}$ ) for all the runs with different  $\alpha_0$ , if the simulation time is long enough. This is a natural equilibrium state and is also expected from equation (1).

Figure 4 displays the electron distribution function  $f(\alpha)$  at  $t = 0.05\Omega_i^{-1}$  for the case  $\alpha_0 = 45^\circ$  in Figure 2. The gray solid line with dots as data marker shows the simulation result, while the black dashed line displays the best Gaussian fit with a mean of  $44.999^\circ$  and a standard deviation of  $1.1515^\circ$ . In the early stage,  $f(\alpha)$  gradually spreads from the initial  $f(\alpha, 0) = \delta(\alpha - \alpha_0)/\sin \alpha_0$ . It maintains an approximate Gaussian shape and very symmetric about  $\alpha_0$ . According to equation (8), the variance of  $f(\alpha)$  increases linearly with time at an approximate rate of  $2D_{\alpha\alpha}(\alpha_0)$ . At  $\alpha_0 = 45^\circ$ , the test particle simulation gives  $D_{\alpha\alpha}(\alpha_0) = 4.3 \times 10^{-3}\Omega_i$ . This corresponds to a variance of  $4.3 \times 10^{-4}$  at  $t = 0.05\Omega_i^{-1}$ , which is equivalent to a standard deviation of  $1.2^\circ$  and very close to the standard deviation of the Gaussian fit in Figure 4.

The discussion about the correlation time,  $\tau_c$ , and the departure time,  $\tau_d$ , in section 2 shows that linear growth of the mean-square pitch-angle change in time can only be expected during the time period,  $\tau_c < t < \tau_d$ . In Figure 2, we can safely take the mean-square pitch-angle changes at the beginning ( $t_1 = 0$ ) and the end ( $t_2 = 2\Omega_i^{-1}$ ) of each run to calculate the pitch-angle diffusion coefficient using equation (9) because  $\tau_c$  is small compared to the chosen  $\Delta t = t_2 - t_1 = 2\Omega_i^{-1}$ . When  $R$  becomes large, it is found that

the correlation time,  $\tau_c$ , and the departure time,  $\tau_d$ , approach each other. Figure 5 shows the time evolution of the mean-square pitch-angle change for electrons with  $\alpha_0 = 45^\circ$  when  $R = 1$ . After an initial period ( $t \leq 0.01\Omega_i^{-1}$ ) of nonlinear growth related to  $\tau_c$ , the mean-square pitch-angle change increases linearly with time and starts to bend over around  $t = 0.025\Omega_i^{-1}$  corresponding to  $\tau_d$ . In this case, the diffusion coefficient has to be calculated strictly from the slope of the linear growth range using equation (9), which gives  $D_{\alpha\alpha} = 1.4\Omega_i$ .

To explore the effect of the wave amplitude on electron scattering, we fix  $\alpha_0$  at  $45^\circ$  and change  $R$  from 0.00001 to 10. The pitch-angle diffusion coefficient at each  $R$  is calculated using equation (9) as discussed above and plotted in Figure 6 (solid line with dots as data marker). Quasi-linear theory predicts that the diffusion coefficient increase with wave spectral density and is proportional to  $R^2$  (shown as dashed line in Figure 6). The test particle simulation results generally agree with quasi-linear theory except at large  $R$  when the wave amplitude is comparable with or greater than the amplitude of the background magnetic field. The discrepancy at large  $R$  is expected because weak turbulence approximation does not hold when the wave amplitude is so large.

#### 4. Discussions

Linear growth in time of the mean-square pitch-angle change can only be expected when  $\tau_c < t < \tau_d$ , but how to exactly determine  $\tau_c$  and  $\tau_d$  remains unknown. If we assume that  $D_{\alpha\alpha}$  has no dependence on pitch angle, the departure of the time evolution of the mean-square pitch-angle change from the linear growth begins when the second term on the right-hand side of equation (7) becomes comparable with the first term. As shown in Figure 4, for  $t < \tau_d$ ,  $f(\alpha)$  slightly spreads from the initial  $f(\alpha, 0) = \delta(\alpha - \alpha_0)/\sin \alpha_0$ , but

maintains an approximate Gaussian shape and is about symmetric about  $\alpha_0$ . Therefore, the ratio of the second term to the first term on the right-hand side of equation (7),

$$\begin{aligned}
& \int_0^\pi (\alpha - \alpha_0) f(\alpha, t) \cos \alpha d\alpha \\
& \approx \int_0^\pi (\alpha - \alpha_0) f(\alpha, t) [\cos \alpha_0 - \sin \alpha_0 (\alpha - \alpha_0)] d\alpha \\
& = \int_0^\pi (\alpha - \alpha_0) f(\alpha, t) \cos \alpha_0 d\alpha \\
& \quad - \int_0^\pi (\alpha - \alpha_0)^2 f(\alpha, t) \sin \alpha_0 d\alpha \\
& \approx 0 - \int_0^\pi (\alpha - \alpha_0)^2 f(\alpha, t) \sin \alpha d\alpha \\
& \approx -2D_{\alpha\alpha}(\alpha_0)t.
\end{aligned} \tag{10}$$

The last step in equation (10) used the approximation that the variance of  $f(\alpha)$  increases linearly with time at a rate of  $2D_{\alpha\alpha}(\alpha_0)$ , according to equation (8). Equation (10) shows that the ratio of the second term to the first term on the right-hand side of equation (7) is negative and its absolute value increases at a rate of  $2D_{\alpha\alpha}(\alpha_0)$  with time. This suggests that  $\tau_d$  is inversely proportional to  $D_{\alpha\alpha}(\alpha_0)$ . From equation (4),  $\tau_d$  would be inversely proportional to the wave spectral density and consequently  $R^2$  in the test particle simulation. If we further define  $\tau_d$  as the time when the ratio of the second term to the first term on the right-hand side of equation (7) is 0.1, then  $\tau_d = 0.1/2D_{\alpha\alpha}(\alpha_0)$ . This gives  $\tau_d = 3.6 \times 10^{-2}\Omega_i^{-1}$  for the case shown in Figure 5. As shown in Figure 5, this is a rather good estimation if we take into account the effect of  $\tau_c$ . In addition, the decrease of the growth rate of the mean-square pitch-angle change at the departure time in Figure 5 is also in agreement with equation (10).

The evaluation of  $\tau_c$  involves statistical analysis and is not well understood. Our preliminary analysis of the test particle simulations shows that  $\tau_c$  decreases with increasing

wave amplitude and seems to suggest that  $\tau_c \propto 1/\sqrt{R}$ . If so,  $\tau_d \propto 1/R^2$  decreases faster than  $\tau_c$  when  $R$  increases.  $\tau_c$  would become comparable with  $\tau_d$  when  $R$  is large enough. When this critical  $R$ , referred to as  $R_C$ , is reached, equation (1) of the pitch-angle diffusion equation is not applicable and quasi-linear theory fails. At the same time, the numerical method proposed in the present study, i.e., using equation (9) to calculate pitch-angle diffusion coefficient, becomes invalid, since the time range of a linear growth of the mean-square pitch-angle change,  $\tau_c < t < \tau_d$ , cannot be found. However, the result in Figure 6 suggests that quasi-linear theory starts to fail before the critical  $R_C$  is reached, possibly owing to the breakdown of the weak turbulence approximation first.

In Figure 1, only wave modes with  $k > k_{min} = 0.42\lambda_i^{-1}$  can resonate with electrons of 2 MeV. Electrons of smaller energy correspond to even larger  $k_{min}$  (for 1 MeV electrons,  $k_{min} = 0.73\lambda_i^{-1}$ ). This implies that geophysically interesting relativistic electrons ( $\leq 2$  MeV) resonate with EMIC waves of relatively large  $k$  only. Linear theory of the ion cyclotron instability [Gary, 1993] shows that the most unstable wavenumber,  $k_0$ , increases with increasing ion temperature anisotropy,  $T_{i\perp}/T_{i\parallel}$ , and decreases with increasing  $\beta_{i\parallel}$ . This suggests that a large  $T_{i\perp}/T_{i\parallel}$  and a small  $\beta_{i\parallel}$  are desirable in order to excite unstable EMIC wave modes which can resonate with geophysically interesting relativistic electrons ( $k_0 > k_{min}$ ). In addition, equation (3) can be written into a dimensionless form,

$$\tilde{k}\tilde{v}_{\parallel}\frac{c}{V_A} = \tilde{\Omega}_e/\gamma, \quad (11)$$

where  $\tilde{k} = k\lambda_i$ ,  $\tilde{v}_{\parallel} = v_{\parallel}/c$ ,  $\tilde{\Omega}_e = \Omega_e/\Omega_i = m_i/m_e$ . By doing this,  $\tilde{\Omega}_e$  is fixed and it is clear that a large  $c/V_A$  can effectively reduce  $k_{min}$ . Since  $\beta_{i\parallel} = n_0T_{i\parallel}/(B_0^2/2\mu_0)$  and  $V_A = B_0/\sqrt{\mu_0n_0m_i}$ ,  $\beta_{i\parallel}$  and  $c/V_A$  both increase as  $n_0/B_0^2$  increases. Consequently, both  $k_0$  and  $k_{min}$  decrease. Fortunately, the dependence of  $k_0$  on  $\beta_{i\parallel}$  is relatively weak. The

net effect of increasing  $n_0/B_0^2$  is the enhancement of the condition  $k_0 > k_{min}$ . To sum up, in the radiation belts, strong pitch-angle diffusion of geophysically interesting relativistic electrons by EMIC waves can be expected in regions of large  $T_{i\perp}/T_{i\parallel}$ , small  $T_{i\parallel}$  and large  $n_0/B_0^2$ . The last criterion, large  $n_0/B_0^2$ , is equivalent to a low value of the parameter  $\alpha^* = \Omega_e^2/\omega_{pe}^2$  in the work of *Summers and Thorne* [2003], where  $\omega_{pe} = \sqrt{n_0 e^2 / \epsilon_0 m_e}$  is the electron plasma frequency. It can be found in regions of high plasma density and low magnetic field, such as the duskside plasmasphere or within detached plasma regions at high L-values, as pointed out by *Summers and Thorne* [2003].

The present study was carried out in 1D, which makes the comparison with quasi-linear theory easier, as the expression for pitch-angle diffusion coefficient from quasi-linear theory becomes difficult to evaluate when waves propagating at arbitrary angles to the background magnetic field are present. Still, it would be interesting to extend the current study beyond 1D. In addition, the present work uses a uniformly-magnetized, homogeneous background plasma, which is also an assumption of quasi-linear theory. When the characteristic scales of the background magnetic field and plasma inhomogeneity are much larger than the relevant EMIC wavelength, one may take the local diffusion coefficients given by quasi-linear theory and may calculate the bounce-averaged and drift-averaged (over MLT) diffusion coefficients [*Lyons et al.*, 1972; *Shprits et al.*, 2006]. This method falls into question when the characteristic scales of the background magnetic field and plasma inhomogeneity become comparable or even smaller than the relevant EMIC wavelength. Using a single wave mode, *Albert and Bortnik* [2009] demonstrated strong nonlinear interaction of relativistic electrons with moderate-amplitude EMIC waves when the inhomogeneity of the background magnetic field is considered. Similarly, *Bortnik*

*et al.* [2008] showed nonlinear interaction of relativistic electrons with large amplitude whistler-mode waves when the background magnetic field and plasma inhomogeneity is included. Of course, their work used a single wave mode only and quasi-linear theory does not apply. This makes the results not straightforward to relate to quasi-linear theory.

## 5. Summary

Relativistic electron scattering has been studied using a hybrid simulation to generate enhanced EMIC waves and a test particle computation to determine the electron response. The one-dimensional, self-consistent hybrid simulation computes the growth of the ion cyclotron instability driven by the ion temperature anisotropy,  $T_{i\perp} > T_{i\parallel}$ . The test particle code follows the motion of relativistic test electron particles in the input EMIC fluctuations. The time evolution of the mean-square pitch-angle change is calculated and used to estimate the pitch-angle diffusion coefficient. The results agree with quasi-linear diffusion theory very well except for very large amplitude waves when the weak turbulence approximation in quasi-linear theory breaks down.

**Acknowledgments.** This work was supported by National Aeronautics and Space Administration grant xxxxxxxx.

## References

- Albert, J. M. (2003), Evaluation of quasi-linear diffusion coefficients for emic waves in a multispecies plasma, *J. Geophys. Res.*, *108*(A6), doi:10.1029/2002JA009792.
- Albert, J. M. (2005), Evaluation of quasi-linear diffusion coefficients for whistler mode waves in a plasma with arbitrary density ratio, *J. Geophys. Res.*, *110*(A03218), doi:10.1029/2004JA010844.

- Albert, J. M., and J. Bortnik (2009), Nonlinear interaction of radiation belt electrons with electromagnetic ion cyclotron waves, *Geophys. Res. Lett.*, *36*(L12110), doi: 10.1029/2009GL038904.
- Anderson, B. J., R. E. Denton, G. Ho, D. C. Hamilton, S. A. Fuselier, and R. J. Strangeway (1996), Observational test of local proton cyclotron instability in the Earth's magnetosphere, *J. Geophys. Res.*, *101*(A10), 21,527.
- Baker, D. N. (2002), How to cope with space weather, *Science*, *297*, doi: 10.1126/science.1074956.
- Birdsall, C. K., and A. B. Langdon (1985), *Plasma Physics Via Computer Simulation*, McGraw-Hill Book Company, New York.
- Boris, J. P. (1970), Relativistic plasma simulation-optimization of a hybrid code, in *Proc. Fourth Conf. Num. Sim. Plasmas*, p. 3, Naval Res. Lab, Washington, D.C.
- Bortnik, J., R. M. Thorne, and U. S. Inan (2008), Nonlinear interaction of energetic electrons with large amplitude chorus, *Geophys. Res. Lett.*, *35*(L21102), doi: 10.1029/2008GL035500.
- Cornwall, J. M. (1965), Cyclotron instabilities and electromagnetic emission in the ultra low frequency and very low frequency ranges, *J. Geophys. Res.*, *70*(1), 61.
- Fraser, B. J., and T. S. Nguyen (2001), Is the plasmopause a preferred source region of electromagnetic ion cyclotron waves in the magnetosphere?, *J. Atmos. Sol. Terr. Phys.*, *63*(11), 1225, doi:10.1016/S1364-6826(00)00225-X.
- Friedel, R. H. W., G. G. Reeves, , and T. Obara (2002), Relativistic electron dynamics in the inner magnetosphere a review, *J. Atmos. Sol. Terr. Phys.*, *64*(2), 265, doi: 10.1016/S1364-6826(01)00088-8.

- Gary, S. P. (1993), *Theory of space plasma microinstabilities*, Cambridge Univ. Press, New York.
- Gary, S. P., and D. Winske (1996), Field/field spatial correlation function: Electromagnetic proton cyclotron instability, *J. Geophys. Res.*, *101*(A2), 2661.
- Gary, S. P., J. Wang, D. Winske, and S. A. Fuselier (1997), Proton temperature anisotropy upper bound, *J. Geophys. Res.*, *102*(A12), 27,159.
- Glauert, S. A., and R. B. Horne (2005), Calculation of pitch angle and energy diffusion coefficients with the padie code, *J. Geophys. Res.*, *110*(A04206), doi: 10.1029/2004JA010851.
- Horne, R. B., and R. M. Thorne (1993), On the preferred source location for the convective amplification of ion cyclotron waves, *J. Geophys. Res.*, *98*(A6), 9233.
- Imhof, W. L. (1968), Electron precipitation in the radiation belts, *J. Geophys. Res.*, *73*(13), 4167.
- Ivanov, E. N. (1965), The general theory of brownian motion, *Soviet Physics Journal*, *8*(6), 35.
- Kennel, C. F., and F. Engelmann (1966), Velocity space diffusion from weak plasma turbulence in a magnetic field, *Phys. Fluids*, *9*(12), 2377.
- Kennel, C. F., and H. E. Petschek (1966), Limit on stably trapped particle fluxes, *J. Geophys. Res.*, *71*(1), 1.
- Lemons, D. S. (2002), *An Introduction to Stochastic Processes in Physics*, Johns Hopkins University Press, Baltimore.
- Lerche, I. (1968), Quasilinear theory of resonant diffusion in a magneto-active, relativistic plasma, *Phys. Fluids*, *11*(8), 1720.

- Lyons, L. R. (1974), Pitch angle and energy diffusion coefficients from resonant interactions with ion-cyclotron and whistle waves, *J. Plasma Phys.*, *12*, 417.
- Lyons, L. R., R. M. Thorne, and C. F. Kennel (1971), Electron pitch angle diffusion driven by oblique whistler-mode turbulence, *J. Plasma Phys.*, *6*, 589.
- Lyons, L. R., R. M. Thorne, and C. F. Kennel (1972), Pitch-angle diffusion of radiation belt electrons within the plasmasphere, *J. Geophys. Res.*, *77*(19), 3455.
- Mauk, B. H., and R. L. McPherron (1980), An experimental test of the electromagnetic ion cyclotron instability within the Earth's magnetosphere, *Phys. Fluids*, *23*(10), 2111, doi:10.1063/1.862873.
- McKean, M. E., D. Winske, and S. P. Gary (1992), Mirror and ion cyclotron anisotropy instabilities in the magnetosheath, *J. Geophys. Res.*, *97*(A12), 19,421.
- McKean, M. E., D. Winske, and S. P. Gary (1994), Two-dimensional simulations of ion anisotropy instabilities in the magnetosheath, *J. Geophys. Res.*, *99*(A6), 11,141.
- Meredith, N. P., R. B. Horne, R. M. Thorne, D. Summers, and R. R. Anderson (2004), Substorm dependence of plasmaspheric hiss, *J. Geophys. Res.*, *109*(A06209), doi:10.1029/2004JA010387.
- Meredith, R. M. T. R. B. H. D. S. B. J. F., N. P., and R. R. Anderson (2003), Statistical analysis of relativistic electron energies for cyclotron resonance with emic waves observed on crres, *J. Geophys. Res.*, *108*(A6), 1250, doi:10.1029/2002JA009700.
- Millan, R. M., and R. M. Thorne (2006), Review of radiation belt relativistic electron losses, *J. Atmos. Sol. Terr. Phys.*, *69*(3), 362, doi:10.1016/j.jastp.2006.06.019.
- Reeves, G. D., K. L. McAdams, R. H. W. Friedel, and T. P. O'Brien (2003), Acceleration and loss of relativistic electrons during geomagnetic storms, *Geophys. Res. Lett.*, *30*,

doi:10.1029/2002GL016513.

Schulz, M., and L. J. Lanzerotti (1974), *Particle Diffusion in the Radiation Belts*, Springer-Verlag, New York.

Selesnick, R. S., J. B. Blake, and R. A. Mewaldt (2003), Atmospheric losses of radiation belt electrons, *J. Geophys. Res.*, *108*(A12), 1468, doi:10.1029/2003JA010160.

Shprits, Y. Y. (2009), Potential waves for pitch-angle scattering of near-equatorially mirroring energetic electrons due to the violation of the second adiabatic invariant, *Geophys. Res. Lett.*, *36*(L12106), doi:10.1029/2009GL038322.

Shprits, Y. Y., R. M. Thorne, R. B. Horne, and D. Summers (2006), Bounce-averaged diffusion coefficients for field-aligned chorus waves, *J. Geophys. Res.*, *111*(A10225), doi:10.1029/2006JA011725.

Summers, D. (2005), Quasi-linear diffusion coefficients for field-aligned electromagnetic waves with applications to the magnetosphere, *J. Geophys. Res.*, *110*(A08213), doi:10.1029/2005JA011159.

Summers, D., and R. M. Thorne (2003), Relativistic electron pitch-angle scattering by electromagnetic ion cyclotron waves during geomagnetic storms, *J. Geophys. Res.*, *108*(A4), 1143, doi:10.1029/2002JA009489.

Summers, D., R. M. Thorne, and F. Xiao (1998), Relativistic theory of wave-particle resonant diffusion with application to electron acceleration in the magnetosphere, *J. Geophys. Res.*, *103*(A9), 20,487.

Thorne, R. M., T. P. O'Brien, Y. Y. Shprits, D. Summers, and R. B. Horne (2005), Timescale for mev electron microburst loss during geomagnetic storms, *J. Geophys. Res.*, *110*(A09202), doi:10.1029/2004JA010882.

Winske, D., and N. Omidi (1993), Hybrid codes: Methods and applications, in *Computer Space Plasma Physics: Simulation Techniques and Software*, edited by H. Matsumoto and Y. Omura, p. 103, Terra Scientific, Tokyo.

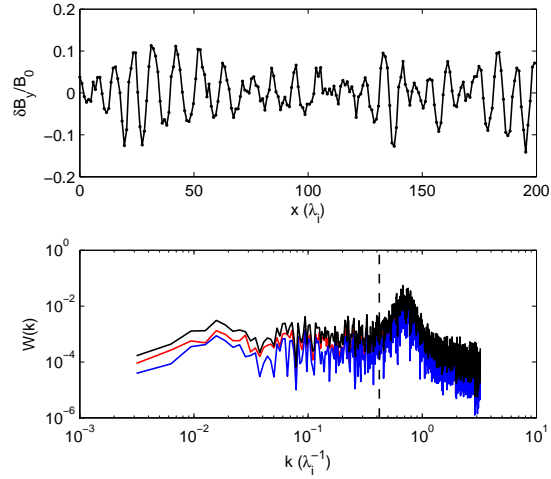


**Figure 1.** The input EMIC waves of the test particle simulation. The top panel displays  $B_y/B_0$  versus  $x$  for  $0 \leq x \leq L_x/10 = 200\lambda_i$  at  $t = 75\Omega_i^{-1}$ . The bottom panel gives the spectral densities for  $B_y$ ,  $B_z$  components and the total EMIC waves (time averaged between  $t = 75\Omega_i^{-1}$  and  $t = 77\Omega_i^{-1}$ , during which the EMIC waves are taken as input for the test particle simulation cases displayed). The vertical dash line marks the wavenumber  $k_{min} = \Omega_e/\gamma v = 0.42\lambda_i^{-1}$  above which the test electrons of 2MeV can resonate with the wave modes. Decided by the resonance condition equation (3), electrons of 2MeV cannot resonate with wave modes  $k < k_{min}$ .

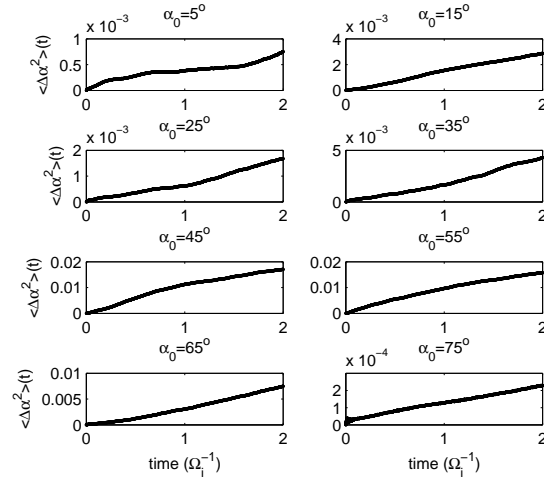


**Figure 2.** The time evolution of the mean-square pitch-angle change for electrons with different initial pitch angle  $\alpha_0$ .

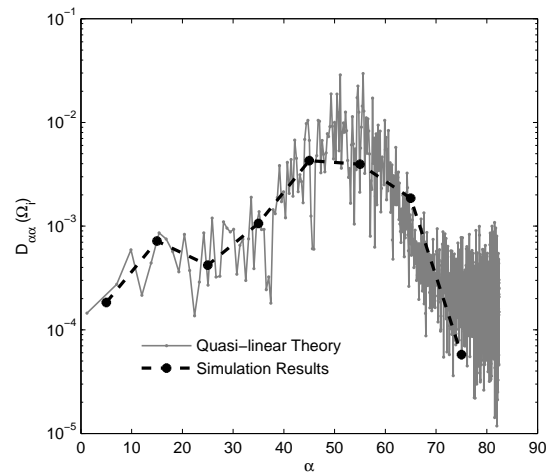


**Figure 3.** The comparison of the pitch-angle diffusion coefficients between quasi-linear theory and simulation results.

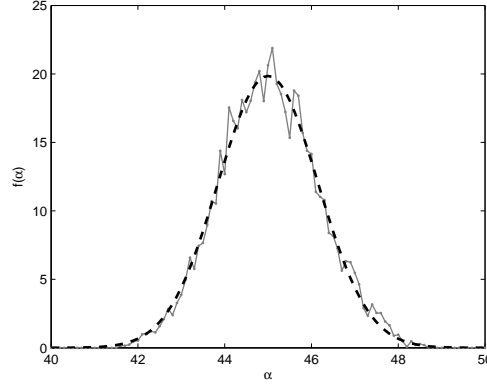


**Figure 4.** The electron distribution function  $f(\alpha)$  at  $t = 0.05$  for the case  $\alpha_0 = 45^\circ$  in Figure 2. The gray solid line with dots as data marker shows the simulation result, while the black dashed line displays the best Gaussian fit with a mean of  $44.999^\circ$  and a standard deviation of  $1.1515^\circ$ .

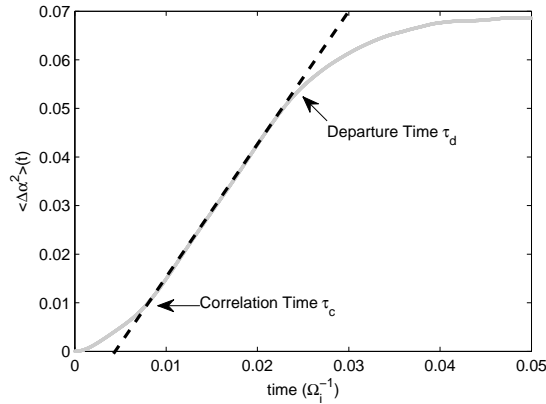


**Figure 5.** The time evolution of the mean-square pitch-angle change for electrons with  $\alpha_0 = 45^\circ$  when  $R = 1$ .

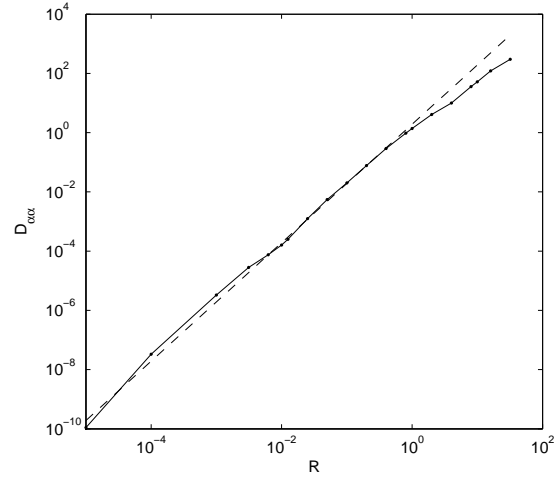


**Figure 6.** The dependence of the pitch-angle diffusion coefficient on the wave amplitude rescaling factor  $R$ . The solid line with dots as data marker shows the test particle simulation results, while the dashed line is from quasi-linear theory.